nature immunology

The scavenger receptor SCARF1 mediates the clearance of apoptotic cells and prevents autoimmunity

Zaida G Ramirez-Ortiz[1], William F Pendergraft III[1–3], Amit Prasad[1], Michael H Byrne[1], Tal Iram[1,4], Christopher J Blanchette[1], Andrew D Luster[1], Nir Hacohen[1,3], Joseph El Khoury[1,5] & Terry K Means[1,3]

The clearance of apoptotic cells is critical for the control of tissue homeostasis; however, the full range of receptors on phagocytes responsible for the recognition of apoptotic cells remains to be identified. Here we found that dendritic cells (DCs), macrophages and endothelial cells used the scavenger receptor SCARF1 to recognize and engulf apoptotic cells via the complement component C1q. Loss of SCARF1 impaired the uptake of apoptotic cells. Consequently, in SCARF1-deficient mice, dying cells accumulated in tissues, which led to a lupus-like disease, with the spontaneous generation of autoantibodies to DNA-containing antigens, activation of cells of the immune system, dermatitis and nephritis. The discovery of such interactions of SCARF1 with C1q and apoptotic cells provides insight into the molecular mechanisms involved in the maintenance of tolerance and prevention of autoimmune disease.

The clearance of apoptotic cells is one of the most important processes of the immune system and is necessary for the homeostatic maintenance of healthy tissues and the removal of infected or damaged cells[1–3]. Several types of cells are able to take up apoptotic cells, including both professional scavengers (macrophages and dendritic cells (DCs)) and nonprofessional phagocytes (fibroblasts, endothelial and epithelial cells). *In vivo*, phagocytes are responsible for the rapid removal of dying cells before necrosis, a post-apoptotic stage accompanied by loss of membrane integrity and leakage of noxious intracellular molecules into the surrounding tissues[4,5]. The phagocyte engulfment of apoptotic cells occurs by an immunologically silent process through the activation of immunosuppressive pathways and the production of anti-inflammatory cytokines to prevent an immune response to self antigens[6]. Consequently, defects in the recognition and/or engulfment of apoptotic cells can lead to chronic inflammatory diseases such as systemic lupus erythematosus (SLE), rheumatoid arthritis, glomerulonephritis and atherosclerosis[7]. Several studies have shown that patients with the autoimmune disease SLE have more circulating apoptotic cells, indicative of a failure in the clearance of dying cells[8]. In addition, patients with lupus have circulating autoantibodies with specificity to intracellular autoantigens, which further emphasizes the importance of the clearance of apoptotic cells in maintaining tolerance and preventing autoimmunity.

During apoptosis, phosphatidylserine is externalized from the inner leaflet of the cell membrane to its outer leaflet, where it serves as a chief recognition and 'eat-me' signal for phagocytes[9]. Several cell-surface receptors (such as TIM-1, TIM-3, TIM-4 and BAI) and soluble bridging proteins (such as MFG-E8, calreticulin and the complement component C1q) can specifically bind to phosphatidylserine exposed on the surface of dying cells and enhance the uptake of apoptotic cells by phagocytes[10–15]. The mechanism used by those bridging molecules awaits further characterization; however, studies have demonstrated that calreticulin acts as an 'eat-me' signal on the surface of apoptotic cells, whereas that signal is overridden on live cells by 'do-not-eat-me' signals involving the signal-regulatory protein CD47 (IAP)[16]. Furthermore, the proposal of an important role for C1q and MFG-E8 in clearance of apoptotic cells is supported by data demonstrating the accumulation of apoptotic cells and the development of lupus-associated autoimmune disease in mice deficient in C1q or MFG-E8 (refs. 17–19). Other studies have demonstrated that C1q, calreticulin and phosphatidylserine have strong interactions with each other and have suggested a combinatorial role for these three molecules in the recognition of apoptotic cells[14]. So far, the identification of the full range of receptors used by phagocytes to recognize and engulf apoptotic cells opsonized by C1q, calreticulin and/or MFG-E8 *in vivo* has remained elusive.

Scavenger receptors are a large family of structurally diverse molecules that have been linked to the recognition of endogenous host-derived ligands and microbial pathogens[20]. SCARF1 (originally called 'scavenger receptor expressed by endothelial cell 1' (SREC-1) after it was cloned from a cDNA library of endothelial cells) is an 86-kilodalton single-pass type 1 transmembrane protein composed of 830 amino acids[21]. The extracellular domain is made up of 406 amino acids and contains five epidermal growth factor (EGF)-like cysteine-rich repeats, followed by a long carboxy-terminal cytoplasmic tail (391 amino acids) composed of serine- and proline-rich regions.

[1]Center for Immunology and Inflammatory Diseases and Division of Rheumatology, Allergy and Immunology, Massachusetts General Hospital and Harvard Medical School, Charlestown, Massachusetts, USA. [2]Division of Nephrology, Massachusetts General Hospital, Boston, Massachusetts, USA. [3]Broad Institute of Harvard and MIT, Cambridge, Massachusetts, USA. [4]Department of Neurobiology, George S. Wise Faculty of Life Sciences, Tel Aviv University, Tel Aviv, Israel. [5]Division of Infectious Diseases, Massachusetts General Hospital, Boston, Massachusetts, USA. Correspondence should be addressed to T.K.M. (means.terry@mgh.harvard.edu).

Received 28 January; accepted 21 June; published online 28 July 2013; doi:10.1038/ni.2670

EGF-like domains mediate homophilic and heterophilic protein-protein interactions, and these domains in SCARF1 have been postulated to contribute to the oligomerization of the protein or to serve as the ligand-binding domain. Although SCARF1 was first shown to bind acetylated low-density lipoprotein (acLDL), SCARF1 is also an endocytic receptor for the heat-shock proteins hsp70, hsp90 and gp96, as well as calreticulin and the pancreatic zymogen GP2 (refs. 22–26). In addition to recognizing those endogenous host proteins, SCARF1 also binds to and is involved in internalizing pathogenic fungi and *Neisseria gonorrhoeae* bacteria through its interaction with gp96 (refs. 27,28).

Scavenger receptors are also present in lower organisms, including the nematode *Caenorhabditis elegans*, which expresses CED-1, a transmembrane receptor that is homologous to mammalian SCARF1, particularly in its extracellular EGF-like cysteine-rich repeat domains, and has an overall similarity of 24% with SCARF1 (refs. 29,30). Published work has reported that CED-1 is required for the capture of necrotic cells in *C. elegans*[29]. Those observations prompted us to generate mice deficient in SCARF1 to determine if this receptor is the mammalian ortholog to CED-1 and shares with it an evolutionarily conserved function in the capture apoptotic cells. Here we found that SCARF1 bound and engulfed apoptotic cells by recognizing C1q bound to phosphatidylserine exposed on the surface of dying cells but not on live cells. Our findings demonstrate a critical evolutionarily conserved role for SCARF1 in removing apoptotic cells and show that its failure can lead to autoimmune disease.

RESULTS

SCARF1 mediates the recognition of dying cells

The *C. elegans* receptor CED-1 and its mammalian ortholog SCARF1 function in innate sensing of the fungal pathogen *Cryptococcus neoformans*[27,30]. To identify other ligands of SCARF1, we constructed a chimera composed of the extracellular domain of SCARF1 fused to the intracellular domain of the TNFRSF1A (TNF-R1) receptor for tumor-necrosis factor (TNF) and expressed the resultant SCARF1–TNF-R1 fusion in HEK293T human embryonic kidney cells (**Supplementary Fig. 1a**). The binding of ligand to the chimeric receptor triggered signaling via the adaptors TRAF2 and RIP1, which led to activation of the transcription factor NF-κB and expression of the gene encoding interleukin 8 (IL-8) in these reporter cells. For example, the addition of heat-killed *C. neoformans* to the reporter cells induced signaling by CED-1–TNF-R1 and mouse SCARF1–TNF-R1 and by a fusion of the fungal β-glucan receptor dectin-1 and TNF-R1 (**Supplementary Fig. 1b**).

To determine whether SCARF1, like CED-1, is involved in the innate recognition of apoptotic cells, we exposed mouse embryonic fibroblasts (MEFs) to ultraviolet irradiation and added the resultant apoptotic 'UV-MEFs' to the reporter cells. We observed activation of reporter cell lines expressing mouse SCARF1–TNF-R1, human SCARF1–TNF-R1 or CED-1–TNF-R1 but not those expressing dectin-1–TNF-R1 (**Fig. 1a**). Furthermore, the activation of cells expressing SCARF1–TNF-R1 correlated with the number of apoptotic cells placed in coculture, but the activation of cells expressing dectin-1–TNF-R1 did not, and the former activation was blocked by the addition of recombinant soluble extracellular human SCARF1 (**Fig. 1b**,**c**). As an additional control, we generated reporter cells expressing human SCARF2, a related member of the scavenger receptor family with 35% amino acid homology to SCARF1 (ref. 31). In contrast to the results obtained for SCARF1, apoptotic cells did not trigger signaling by SCARF2–TNF-R1 reporter cells (**Fig. 1b**), which indicated the specificity of SCARF1 in the sensing of apoptotic cells. By a conventional flow cytometry assay, we found that cells expressing SCARF1–TNF-R1 captured dye-labeled UV-MEFs, but those expressing dectin-1–TNF-R1 did not (**Fig. 1c**), which indicated a direct interaction between SCARF1 and apoptotic cells. Microscopic analysis of cells expressing SCARF1–TNF-R1 showed binding to apoptotic cells,

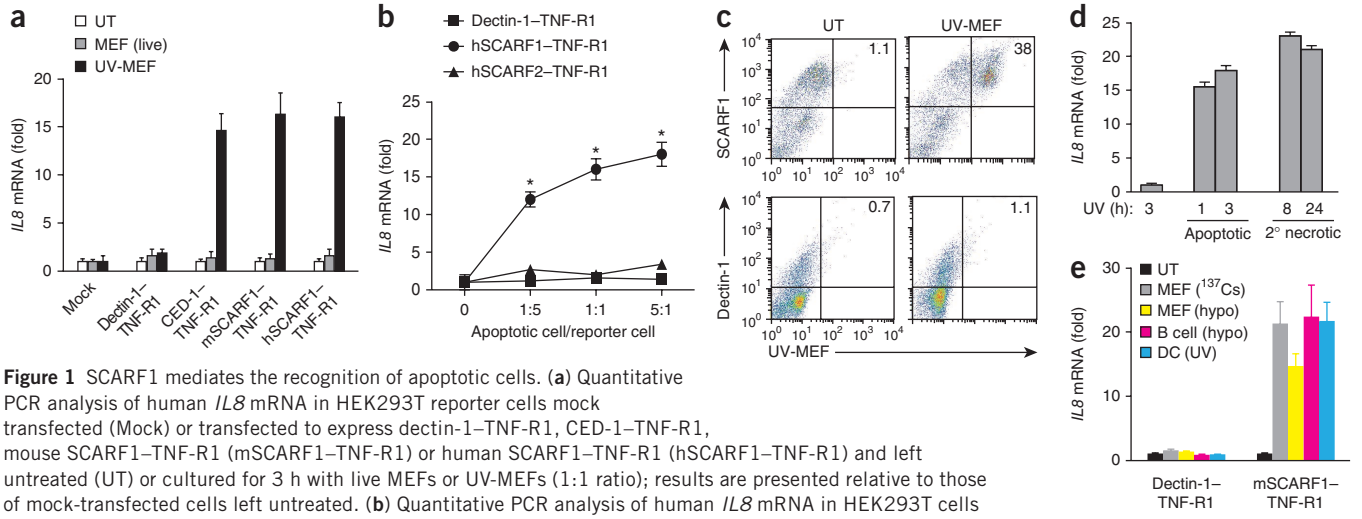

Figure 1 SCARF1 mediates the recognition of apoptotic cells. (**a**) Quantitative PCR analysis of human *IL8* mRNA in HEK293T reporter cells mock transfected (Mock) or transfected to express dectin-1–TNF-R1, CED-1–TNF-R1, mouse SCARF1–TNF-R1 (mSCARF1–TNF-R1) or human SCARF1–TNF-R1 (hSCARF1–TNF-R1) and left untreated (UT) or cultured for 3 h with live MEFs or UV-MEFs (1:1 ratio); results are presented relative to those of mock-transfected cells left untreated. (**b**) Quantitative PCR analysis of human *IL8* mRNA in HEK293T cells transfected to express dectin-1–TNF-R1, human SCARF1–TNF-R1 or human SCARF2–TNF-R1 and cultured for 3 h with UV-MEFs (ratio, horizontal axis), assessed and presented as in **a**. (**c**) Capture of MEFs by HEK293T reporter cells transfected to express mouse SCARF1–TNF-R1 (top) or dectin-1–TNF-R1 (bottom) and left untreated or cultured for 3 h with dye-labeled apoptotic UV-MEFs (1:1 ratio), analyzed flow cytometry. Numbers in top right quadrants indicate percent reporter cells that captured apoptotic UV-MEFs. (**d**) Quantitative PCR analysis of human *IL8* mRNA in HEK293T reporter cells transfected to express mouse SCARF1–TNF-R1 and cultured for 3 h at a ratio of 1:1 with live MEFs (far left) or with UV-MEFs that had been allowed to 'rest' in culture for 1 or 3 h (early apoptotic cells (Apoptotic); annexin V positive and propidium iodide negative) or for 8 or 24 h (secondary necrosis (2° necrotic); positive for annexin V and propidium iodide) after ultraviolet irradiation (assessed and presented as in **a**). (**e**) Quantitative PCR analysis of human *IL8* mRNA in HEK293T reporter cells transfected to express dectin-1–TNF-R1 or mouse SCARF1–TNF-R1 and left untreated or cultured for 3 h at a ratio of 1:1 with apoptotic MEFs irradiated with ^{137}Cs (MEF (^{137}Cs)), MEFs (MEF (hypo)) or primary B cells (B cell (hypo)) treated with hypotonic buffers, or DCs exposed to ultraviolet irradiation (DC (UV)), assessed and presented as in **a**. *$P < 0.001$ (Student's *t*-test). Data are from one experiment representative of at least three experiments (error bars (**a**,**b**,**d**,**e**), mean and s.d. of at least triplicates).

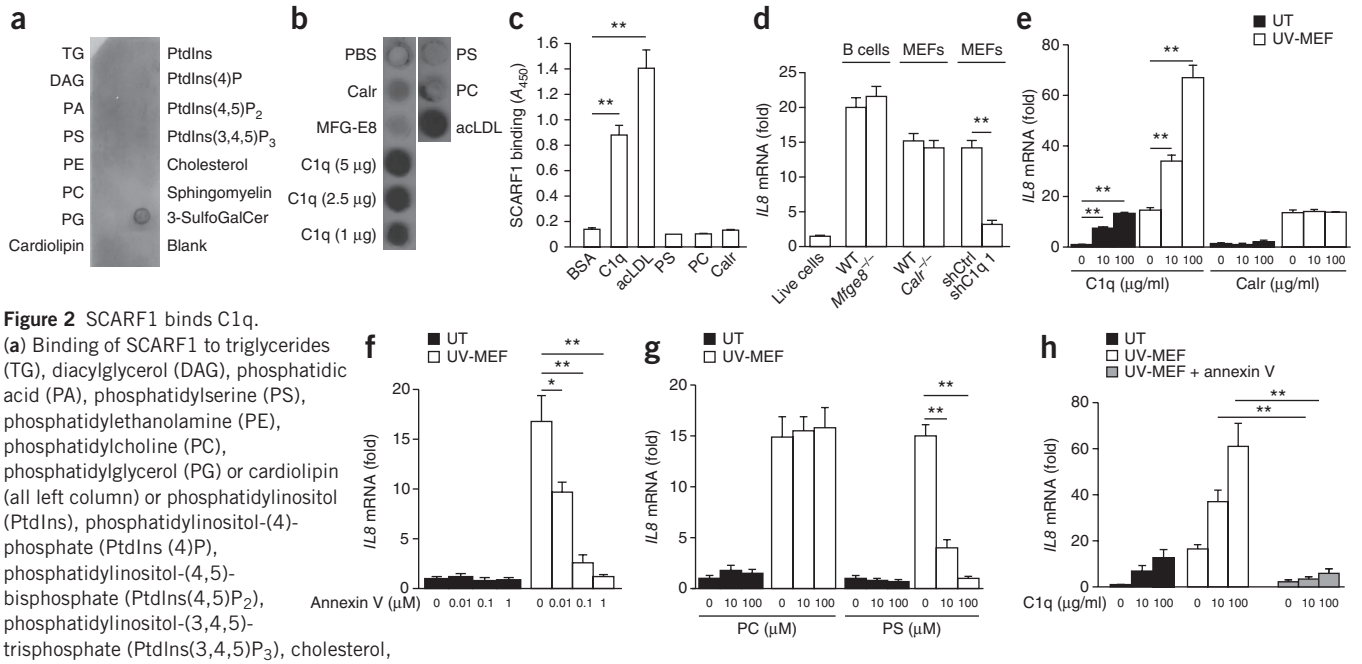

Figure 2 SCARF1 binds C1q. (**a**) Binding of SCARF1 to triglycerides (TG), diacylglycerol (DAG), phosphatidic acid (PA), phosphatidylserine (PS), phosphatidylethanolamine (PE), phosphatidylcholine (PC), phosphatidylglycerol (PG) or cardiolipin (all left column) or phosphatidylinositol (PtdIns), phosphatidylinositol-(4)-phosphate (PtdIns (4)P), phosphatidylinositol-(4,5)-bisphosphate (PtdIns(4,5)P_2), phosphatidylinositol-(3,4,5)-trisphosphate (PtdIns(3,4,5)P_3), cholesterol, sphingomyelin, 3-sulfogalactosylceramide (3-SulfoGalCer) or vehicle (Blank; all right column). (**b**) Binding of SCARF1 to PBS, immobilized calreticulin (Calr), MFG-E8, various concentrations of C1q (all left column) or phosphatidylserine, phosphatidylcholine or acLDL (all right column). (**c**) ELISA of the binding of SCARF1 to BSA, C1q, acLDL, phosphatidylserine, phosphatidylcholine or calreticulin, presented as absorbance at 450 nm (A_{450}). (**d**) Quantitative PCR analysis of human *IL8* mRNA (assessed and presented as in **Fig. 1a**) in HEK293T reporter cells transfected to express mouse SCARF1–TNF-R1 and cultured for 3 h with live cells from C57BL/6 mice (far left), apoptotic B cells from *Mfge8*$^{+/+}$ (WT) or *Mfge8*$^{-/-}$ mice (middle left), apoptotic calreticulin-sufficient (WT) or calreticulin-deficient (*Calr*$^{-/-}$) MEFs (middle right), or apoptotic wild-type MEFs transduced with shRNA targeting green fluorescent protein (GFP; shCtrl) or C1q (shC1q 1 (far right); quantitative PCR analysis of C1q mRNA to assess knockdown efficiency, **Supplementary Fig. 2c**). (**e**–**g**) Quantitative PCR analysis of human *IL8* mRNA (assessed and presented as in **Fig. 1a**) in HEK293T reporter cells transfected to express mouse SCARF1–TNF-R1, then incubated with various concentrations (horizontal axes) of recombinant C1q or calreticulin (**e**), annexin V (**f**) or liposomes containing phosphatidylcholine or phosphatidylserine (**g**) and then left untreated or cultured for 3 h with UV-MEFs. (**h**) Quantitative PCR analysis of human *IL8* mRNA (as in **e**–**g**) in HEK293T reporter cells transfected to express mouse SCARF1–TNF-R1, then incubated with various concentrations of recombinant C1q and then left untreated or cultured for 3 h with UV-MEFs alone or UV-MEFs treated with annexin V. $*P < 0.001$ and $**P < 0.0001$ (Student's *t*-test). Data are from one experiment representative of three independent experiments (**a**,**b**) or one experiment representative of at least three experiments (**c**–**h**; error bars, mean and s.d. of triplicates).

but only cells expressing full-length SCARF1 engulfed apoptotic cells by phagocytosis (data not shown), which indicated that the carboxy-terminal cytoplasmic tail of SCARF1 was needed to signal the actin cytoskeleton for internalization.

As live cells did not trigger SCARF1 signaling (**Fig. 1a**), we sought to determine at what apoptotic stage ligands for SCARF1 were exposed on dying cells. We found that both early apoptotic cells (1–3 h after ultraviolet irradiation) and late apoptotic cells (8–24 h after ultraviolet irradiation) that had undergone secondary necrosis, as assessed by permeability to the DNA stain propidium iodide, triggered SCARF1–TNF-R1 signaling (**Fig. 1d**), which indicated that ligands for SCARF1 were exposed soon after cell death. We also found that SCARF1 signaling was independent of the method used to induce cell death. We induced death in MEFs by osmotic shock or exposure to ^{137}Cs (γ-irradiation) and found that the addition of those dying to the reporter cells induced SCARF1–TNF-R1 signaling similar to the addition of UV-MEFs (**Fig. 1e**). Moreover, all apoptotic cell types tested (B cells, DCs, splenocytes and MEFs), regardless of the species of origin, induced SCARF1–TNF-R1 signaling (**Fig. 1e** and data not shown), which indicated that the ligand was not restricted to the cell type or species. MFG-E8 has been shown to bind to apoptotic cells and facilitate their clearance through interaction with phagocytes[18]. We found that treatment of the reporter cells with recombinant MFG-E8 alone or in combination with apoptotic cells did not trigger or enhance SCARF1–TNF-R1 signaling (**Supplementary Fig. 1c**), which indicated that MFG-E8 was not a ligand for SCARF1. Together these data demonstrated that the CED-1-like scavenger receptor SCARF1 shared an evolutionarily conserved function with CED-1 in the recognition of apoptotic cells.

SCARF1 binds to C1q

The exposure of phosphatidylserine on the outer leaflet of the plasma membrane of apoptotic cells is considered to be the main 'eat-me' signal recognized by phagocytes[9]. As signaling via SCARF1 and binding of SCARF1 to apoptotic cells coincided with their rapid exposure of phosphatidylserine, we hypothesized that phosphatidylserine is a ligand of SCARF1. To examine direct interactions between SCARF1 and phosphatidylserine, we used a protein-lipid overlay dot-blot assay in which we spotted hydrophobic membranes with 15 different lipids present in cell membranes and then probed the membranes with SCARF1 protein. In contrast to MFG-E8, SCARF1 did not bind to phosphatidylserine or any other lipids, except 3-sulfogalactosylceramide, a known ligand of scavenger receptors[32] (**Fig. 2a** and **Supplementary Fig. 2a**). To determine whether the recognition of apoptotic cells by SCARF1 was mediated by 3-sulfogalactosylceramide, we added UV-MEFs to reporter cells expressing SCARF1–TNF-R1, in the presence of 3-sulfogalactosylceramide. We observed that 3-sulfogalactosylceramide did not enhance or inhibit the activation of SCARF1 by apoptotic cells (**Supplementary Fig. 2b**), which indicated that 3-sulfogalactosylceramide (sulfatide) was not an important contributor to the SCARF1–apoptotic cell interactions.

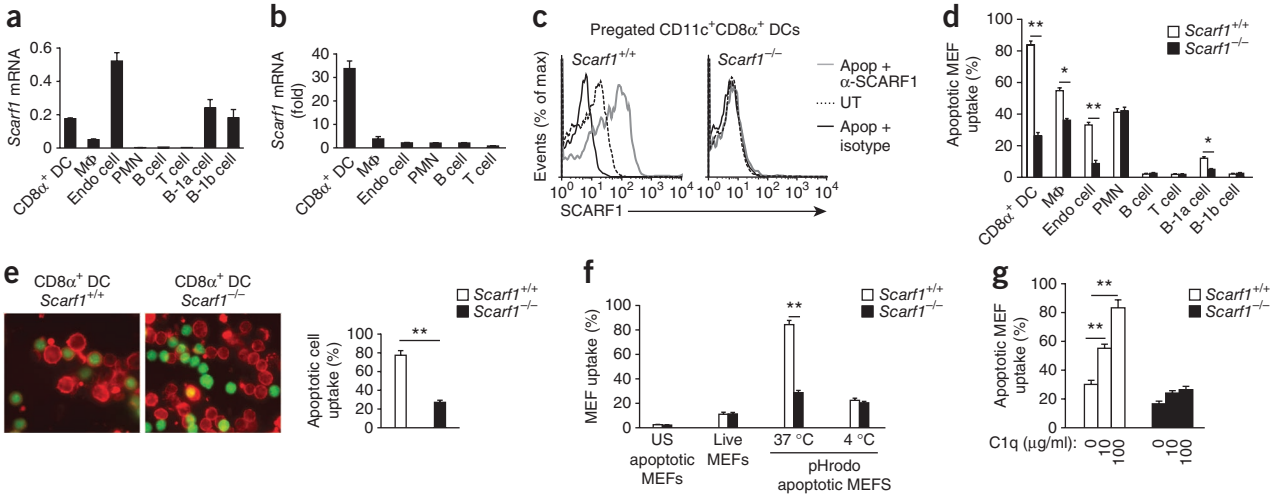

Figure 3 Impaired engulfment of apoptotic cells by SCARF1-deficient CD8α+ DCs. (**a**) Quantitative PCR analysis of *Scarf1* mRNA in CD8α+ DCs, macrophages (MΦ), endothelial cells (Endo cell), polymorphonuclear cells (PMN), B cells, T cells (spleen), neutrophils (bone marrow) and B-1a and B-1b cells (peritoneum) isolated from *Scarf1*$^{+/+}$ mice; results were normalized to those of *B2m* (encoding β_2-microglobulin). (**b**) Quantitative PCR analysis of *Scarf1* mRNA in the cells in **a** after culture for 3 h with *Scarf1*$^{-/-}$ apoptotic B cells; results are presented relative to those of untreated cells. (**c**) Flow cytometry of *Scarf1*$^{+/+}$ and *Scarf1*$^{-/-}$ splenic DCs left untreated and stained with fluorescence-conjugated anti-SCARF1 (UT) or cultured *in vitro* for 4 h with apoptotic *Scarf1*$^{-/-}$ B cells and then stained with fluorescence-conjugated anti-SCARF1 (Apop + α-SCARF1) or isotype-matched control antibody (Apop + isotype); assessed after pregating as CD11c+CD8α+ DCs. (**d**) Uptake of apoptotic MEFs by cells (horizontal axis) isolated from *Scarf1*$^{+/+}$ or *Scarf1*$^{-/-}$ mice ($n = 8$ per group) and incubated for 2 h with dye-labeled apoptotic MEFs, assessed by flow cytometry. (**e**) Confocal microscopy (left) of CD11c+CD8α+ DCs (red) isolated from spleens of *Scarf1*$^{+/+}$ and *Scarf1*$^{-/-}$ mice ($n = 4$ per genotype) by magnetic selection and incubated for 2 h with dye-labeled apoptotic B cells (green), and quantification (right) of DCs that phagocytosed apoptotic cells (in five randomly selected high-power views per slide. Original magnification (left), ×40. (**f**) Uptake of MEFs by CD8α+ DCs cultured for 2 h at 37 °C with unstained (US) apoptotic MEFs (far left) or live MEFs (middle left) or for 2 h at 37 °C (middle right) or 4 °C (far right) with pHrodo-labeled MEFs, assessed by staining for CD11c and CD8α and flow cytometry. (**g**) Uptake of MEFs by *Scarf1*$^{+/+}$ and *Scarf1*$^{-/-}$ splenic CD8α+ DCs cultured for 2 h at 37 °C in C1q-depleted serum with dye-labeled apoptotic UV-MEFs in the presence of various concentrations (horizontal axis) of exogenous C1q, assessed by flow cytometry. $*P < 0.01$ and $**P < 0.001$ (Student's *t*-test). Data are from three independent experiments (**a**,**b**), are representative of four experiments (**c**), five experiments (**d**,**e**) or three experiments (**f**,**g**) or are from one experiment representative of at least three experiments (error bars (**a**,**b**,**d**–**g**), mean and s.d.).

In addition to phosphatidylserine, several soluble bridging proteins have been shown to be involved in the recognition of apoptotic cells, including C1q, calreticulin and MFG-E8 (refs. 12,16,19). Through the use of a protein-protein overlay dot-blot assay, we found that SCARF1 specifically bound to C1q in a concentration-dependent manner, but did not bind to calreticulin or MFG-E8 (**Fig. 2b**). We further examined the direct binding of SCARF1 to C1q by antigen-capture enzyme-linked immunosorbent assay (ELISA) with C1q-coated microtiter plate wells. These experiments showed strong binding of SCARF1 to C1q and to the classic scavenger receptor ligand acLDL, but negligible binding of SCARF1 to bovine serum albumin (BSA), phosphatidylserine, phosphatidylcholine or calreticulin (**Fig. 2c**). Moreover, we observed a similar interaction pattern by ELISA in the reverse configuration, with C1q binding to plate-bound SCARF1 (data not shown). To confirm those findings and determine the affinity of the SCARF1-C1q interaction, we assessed the binding of SCARF1 to a C1q-immobilized sensor chip by measuring surface plasmon resonance. We observed no binding of SCARF1 to phosphatidylserine or calreticulin; however, we noted an affinity dissociation constant of 1.24×10^{-7} M for the interaction of SCARF1 and C1q. These results identified C1q as a ligand for SCARF1.

SCARF1 recognizes dying cells via C1q-phosphatidylserine

To further investigate the interaction of SCARF1 with ligands on apoptotic cells, we cultured reporter cells expressing SCARF1–TNF-R1 with apoptotic cells deficient in C1q, MFG-E8 or calreticulin. Apoptotic cells deficient in C1q were significantly impaired in their ability to induce SCARF1 signaling, but those deficient in MFG-E8 or calreticulin were not (**Fig. 2d** and **Supplementary Fig. 2c**). In addition, C1q alone or in the presence of apoptotic cells triggered SCARF1 signaling (*Il8* expression) in a concentration-dependent manner (**Fig. 2e**). In contrast, treatment with calreticulin was not sufficient to enhance or inhibit the SCARF1-mediated recognition of apoptotic cells (**Fig. 2e**). Together these data demonstrated that the recognition of apoptotic cells by SCARF1 required C1q.

As C1q has been shown to interact with phosphatidylserine on apoptotic cells, we hypothesized that the recognition of apoptotic cells by SCARF1 occurred via a C1q–phosphatidylserine–apoptotic cell interaction[13]. To test our hypothesis, we cultured reporter cells with apoptotic MEFs pretreated with annexin V, a phospholipid-binding protein with high affinity for phosphatidylserine, which binds to exposed phosphatidylserine on apoptotic cells. Pretreatment of apoptotic MEFs with annexin V, which blocked phosphatidylserine, inhibited the signaling of reporter cells expressing SCARF1–TNF-R1 and did so in a dose-dependent manner (**Fig. 2f**). Moreover, to further determine whether the recognition of apoptotic cells by SCARF1 required phosphatidylserine, we did a liposome competition experiment. Liposomes containing phosphatidylserine inhibited apoptotic MEF–induced SCARF1–TNF-R1 signaling in a dose-dependent manner, but liposomes containing phosphatidylcholine did not; however, treatment with phosphatidylserine alone did not activate SCARF1 signaling (**Fig. 2g**). Finally, to determine whether the SCARF1–C1q–apoptotic cell interaction was dependent on phosphatidylserine, we cultured reporter cells expressing SCARF1–TNF-R1 together with annexin V–treated apoptotic MEFs in the presence of C1q. We found that annexin V–treated apoptotic

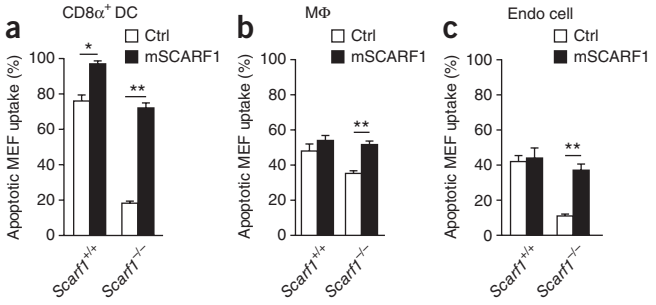

Figure 4 SCARF1 is necessary for the uptake of apoptotic cells. Uptake of apoptotic MEFs by GFP+ *Scarf1*$^{+/+}$ and *Scarf1*$^{-/-}$ splenic CD8α+ DCs (**a**), macrophages (**b**) or endothelial cells (**c**) transfected by nucleofection with vector encoding GFP alone (Ctrl) or a fusion of mouse SCARF1 with GFP at the carboxyl terminus (mSCARF1) and cultured for 2 h at 37 °C with dye-labeled apoptotic MEFs. SCARF1 expression (assessed as GFP expression) was confirmed by flow cytometry, immunoblot analysis and microscopy (not shown). *$P < 0.01$ and **$P < 0.001$ (Student's *t*-test). Data are from one experiment representative of at least three experiments (error bars, mean and s.d. of triplicates).

MEFs did not activate SCARF1-dependent signaling, even in the presence of C1q (**Fig. 2h**). Together these results demonstrated that the SCARF1-mediated recognition of apoptotic cells occurred by the binding of SCARF1 to C1q via phosphatidylserine exposed on apoptotic cells.

SCARF1 mediates the recognition of apoptotic cells *in vitro*

To determine where SCARF1 might serve its function, we did quantitative real-time PCR analysis to examine its expression in various organs of mice (**Supplementary Fig. 3a**). SCARF1 was expressed in a variety of organs, mainly in the spleen and lungs. Expression of SCARF1 was very low in circulating cells of the immune system (neutrophils, T cells and B cells; **Fig. 3a**), consistent with published reports demonstrating its restricted expression on endothelial cells, DCs and macrophages[21,22,26,30] . We also observed SCARF1 expression in peritoneal B-1a and B-1b cells equivalent to that in CD8α+ DCs (**Fig. 3a**). The addition of apoptotic cells to the cell culture medium resulted in higher expression of *Scarf1* mRNA and higher surface expression of SCARF1 protein by CD8α+ DCs, but not by other cell types (**Fig. 3b**,**c**). The CD8α+ DC subset is specialized in capturing dying cells[33], so to further examine the role of SCARF1 in mediating the recognition of and responses to apoptotic cells, we generated SCARF1-deficient (*Scarf1*$^{-/-}$) mice in which SCARF1 expression was ablated by replacement of exons 1–8, which encode the entire extracellular and transmembrane domains, with a neomycin-resistance cassette (**Supplementary Fig. 4a–c**). To determine whether SCARF1 expression on CD8α+ DCs was necessary for the capture and engulfment of apoptotic cells, we used flow cytometry to assess the frequency of the capture of dye-labeled apoptotic cells by CD8α+ DCs isolated from *Scarf1*$^{+/+}$ and *Scarf1*$^{-/-}$ mice. CD8α+ DCs from *Scarf1*$^{-/-}$ mice were significantly less able to acquire dye-labeled apoptotic cells than were *Scarf1*$^{+/+}$ CD8α+ DCs (**Fig. 3d**). These data demonstrated that SCARF1 was required for the recognition of apoptotic cells by CD8α+ DCs. In addition to CD8α+ DCs, *Scarf1*$^{-/-}$ macrophages, endothelial cells and B-1a cells, but not neutrophils, B cells, T cells or B-1b cells, had significant impairment in their uptake of apoptotic cells, consistent with the expression of SCARF1 on these cell types (**Fig. 3d**). These data showed that SCARF1 expression contributed approximately 70%, 32%, 74% and 52% to the clearance of apoptotic cells by CD8α+ DCs, macrophages, endothelial cells and B-1a cells, respectively. As SCARF1 expression provided only a moderate contribution to the uptake of apoptotic cells by macrophages, these results suggested that other pathways for the clearance of apoptotic cells have a more dominant role in this cell type. Indeed, expression of receptors known to be involved in the recognition of apoptotic cells (MFG-E8, TIM-4, CD91 (LRP1), c-Mer and ITAGV) was significantly higher in macrophages than in CD8α+ DCs or endothelial cells ($P < 0.001$; **Supplementary Fig. 3b**), which suggested that these pathways may have partially compensated for the lack of SCARF1.

As a control and to determine whether SCARF1 is a ligand for itself, we cultured *Scarf1*$^{+/+}$ CD8α+ DCs together with apoptotic cells isolated from *Scarf1*$^{+/+}$ and *Scarf1*$^{-/-}$ mice. *Scarf1*$^{+/+}$ CD8α+ DCs engulfed an equivalent percentage of *Scarf1*$^{+/+}$ and *Scarf1*$^{-/-}$ apoptotic cells (data not shown), which indicated that one of the shared ligands of SCARF1 on apoptotic cells was not SCARF1 itself. To confirm the uptake of apoptotic cells, we used confocal microscopy of CD8α+ DCs incubated with dye-labeled apoptotic B cells. *Scarf1*$^{+/+}$ CD8α+ DCs engulfed apoptotic cells and cleared them from the culture medium, but their *Scarf1*$^{-/-}$ counterparts did not (**Fig. 3e**). To further confirm the impairment in the internalization of apoptotic cells by *Scarf1*$^{-/-}$ CD8α+ DCs, we incubated CD8α+ DCs with apoptotic cells labeled with pHrodo, a pH-sensitive fluorescent dye that makes engulfed cells highly fluorescent. *Scarf1*$^{-/-}$ CD8α+ DCs showed a substantial inability to engulf pHrodo-labeled apoptotic cells (**Fig. 3f**). In contrast, *Scarf1*$^{+/+}$ and *Scarf1*$^{-/-}$ CD8α+ DCs engulfed an equivalent, but small, percentage of pHrodo-labeled live cells. To further test our hypothesis that SCARF1 mediates the recognition of apoptotic cells via C1q, we incubated *Scarf1*$^{+/+}$ and *Scarf1*$^{-/-}$ CD8α+ DCs with dye-labeled apoptotic cells in the presence or absence of C1q. C1q significantly enhanced the uptake of apoptotic cells by *Scarf1*$^{+/+}$ CD8α+ DCs but not by *Scarf1*$^{-/-}$ CD8α+ DCs (**Fig. 3g**). Together these experiments indicated that SCARF1 was required for optimal capture of apoptotic cells and was able to specifically 'sense' exposed ligands on apoptotic cells versus live cells.

The recognition of apoptotic cells requires SCARF1

To confirm that the deficiency in the clearance of apoptotic cells by SCARF1-deficient cells was not due to a secondary defect unrelated to the ablation of SCARF1, we reconstituted *Scarf1*$^{-/-}$ CD8α+ DCs, macrophages and endothelial cells with mouse *Scarf1* cDNA through nucleofection. Ectopic expression of *Scarf1*, which we confirmed by immunoblot analysis and microscopy, restored the ability of *Scarf1*$^{-/-}$ CD8α+ DCs, macrophages and endothelial cells to efficiently capture apoptotic cells (**Fig. 4** and data not shown). Moreover, *Scarf1*$^{+/+}$ CD8α+ DCs transfected with mouse *Scarf1* cDNA had >25% more uptake of apoptotic cells than did mock-transfected *Scarf1*$^{+/+}$ CD8α+ DCs (**Fig. 4a**), which indicated that upregulation and/or overexpression of *Scarf1* may be a useful therapeutic strategy for the clearance of dead cells that occurs in some diseases[1].

SCARF1 mediates the clearance of apoptotic cells *in vivo*

To determine whether SCARF1 is necessary for the engulfment of apoptotic cells *in vivo*, we gave *Scarf1*$^{+/+}$ and *Scarf1*$^{-/-}$ mice intravenous injection of dye-labeled apoptotic B cells or 1 μM latex spheres labeled with fluorescein isothiocyanate (FITC), as described[33]. We treated B cells with ultraviolet irradiation to induce apoptosis, which we confirmed by positive staining for annexin V and negative staining for propidium iodide. At 1 h after injecting apoptotic cells or FITC–latex beads, we collected spleens and enriched them for DCs through the use of magnetic microbeads coated with antibody

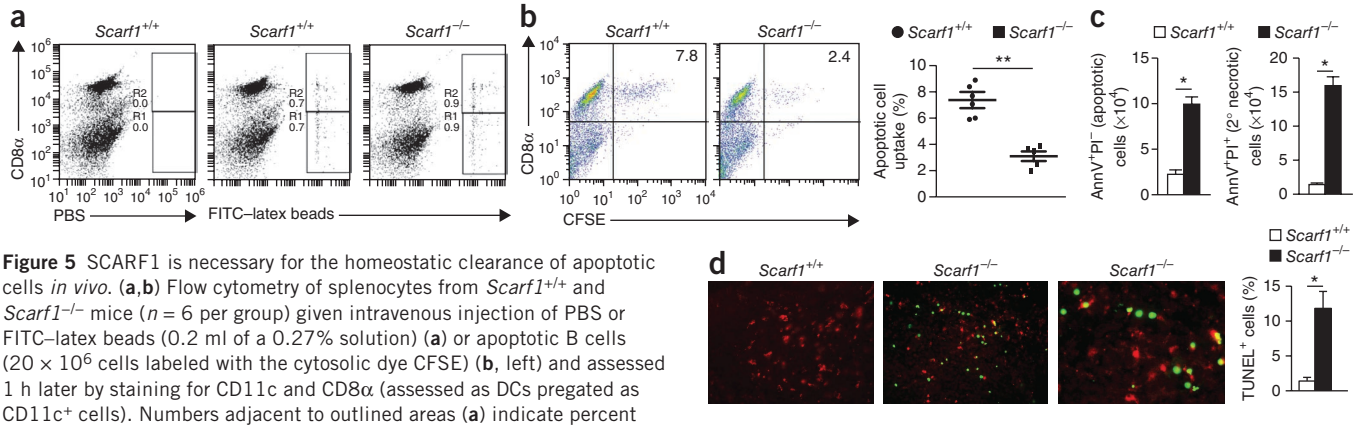

Figure 5 SCARF1 is necessary for the homeostatic clearance of apoptotic cells *in vivo*. (**a**,**b**) Flow cytometry of splenocytes from *Scarf1*$^{+/+}$ and *Scarf1*$^{-/-}$ mice ($n = 6$ per group) given intravenous injection of PBS or FITC–latex beads (0.2 ml of a 0.27% solution) (**a**) or apoptotic B cells (20×10^6 cells labeled with the cytosolic dye CFSE) (**b**, left) and assessed 1 h later by staining for CD11c and CD8α (assessed as DCs pregated as CD11c$^+$ cells). Numbers adjacent to outlined areas (**a**) indicate percent CD8α$^+$ DCs (R2; top) or CD8α$^-$ DCs (R1; bottom); numbers in top right quadrants (**b**) indicate percent CD8α$^+$ DCs that captured apoptotic B cells (CFSE$^+$). Right (**b**), quantification of the uptake of apoptotic B cells by CD11c$^+$CD8α$^+$ splenic DCs: each symbol represents an individual mouse ($n = 5$ per group); small horizontal lines indicate the mean (± s.e.m.). (**c**) Flow cytometry of PBMCs isolated by Ficoll gradients from whole blood of >16-week-old *Scarf1*$^{+/+}$ and *Scarf1*$^{-/-}$ mice ($n = 8$ per group) and stained with annexin V (AnnV) and propidium iodide (PI), presented as total circulating apoptotic cells (left) or secondary necrotic cells (right) per ml blood. (**d**) Fluorescence microscopy (left) of spleen sections from >16-week-old *Scarf1*$^{+/+}$ and *Scarf1*$^{-/-}$ mice, showing apoptotic cells stained by TUNEL (green) and DCs stained with anti-CD11c (red), and quantification of images at left by automated analysis of staining with the nuclear dye DAPI and by TUNEL (right). $^*P < 0.001$, $^{**}P < 0.0001$; Student's *t*-test. Data are representative of three experiments (**a**) or four experiments (**b**), are from three independent experiments (**c**; mean and error bars, s.e.m.) or are representative of three independent experiments with four mice per group (**d**; error bars, s.e.m.).

to CD11c (anti-CD11c). We then used flow cytometry with anti-CD11c and anti-CD8α to identify DCs that had captured apoptotic cells or FITC–latex beads. CD8α$^+$ and CD8α$^-$ DCs from *Scarf1*$^{+/+}$ and *Scarf1*$^{-/-}$ mice captured equivalent amounts of FITC–latex beads (**Fig. 5a**). In contrast, apoptotic cells were engulfed selectively by the CD8α$^+$ DC subset (**Fig. 5b**). Moreover, CD8α$^+$ DCs from *Scarf1*$^{-/-}$ mice captured significantly fewer apoptotic cells than did those from *Scarf1*$^{+/+}$ mice (**Fig. 5b**). These data demonstrated that SCARF1 was necessary on CD8α$^+$ DCs for their capture of dying cells and that SCARF1 may be involved in the homeostatic clearance of apoptotic cells *in vivo*.

To test that hypothesis, we isolated peripheral blood mononuclear cells from the whole blood of 20-week-old *Scarf1*$^{+/+}$ and *Scarf1*$^{-/-}$ mice. We then stained cells with annexin V and propidium iodide and used flow cytometry to quantify circulating apoptotic and necrotic cells. We found significantly more early apoptotic cells (positive for annexin V and negative for propidium iodide) and secondary necrotic cells (positive for annexin V and propidium iodide)—over fourfold and tenfold more, respectively—in the circulation of *Scarf1*$^{-/-}$ mice than in that of *Scarf1*$^{+/+}$ mice (**Fig. 5c**), which indicated an important role for SCARF1 in maintaining the clearance of apoptotic cells *in vivo*.

In wild-type mice, the removal of apoptotic cells is usually a very efficient process, and few apoptotic cells are found even in tissues with a high rate of cell death. However, dying cells accumulated in the tissues of *Scarf1*$^{-/-}$ mice (**Fig. 5d** and data not shown). Notably, spleens from *Scarf1*$^{-/-}$ mice had significantly more apoptotic cells, as assessed by the TUNEL cell-death assay, than did spleens from *Scarf1*$^{+/+}$ mice, and although splenic CD11c$^+$ DCs in *Scarf1*$^{-/-}$ mice were located near apoptotic cells, they had less uptake of those cells than did their *Scarf1*$^{+/+}$ counterparts (**Fig. 5d**). To ensure that the accumulation of apoptotic cells in *Scarf1*$^{-/-}$ mice was due solely to the impairment in clearance of apoptotic cells and was not due to more cell turnover, we monitored the rate of apoptosis of *Scarf1*$^{+/+}$ and *Scarf1*$^{-/-}$ cells. The rate and frequency of apoptosis of *Scarf1*$^{-/-}$ splenocytes, B cells and bone marrow cells was similar to that of *Scarf1*$^{+/+}$ cells (**Supplementary Fig. 5a–c**). Furthermore, the expression of other receptors known to be involved in the recognition of apoptotic cells (C1q, MFG-E8, TIM-1, TIM-3, TIM-4, CD91, MARCO, CD14, LOX-1, SR-A1, GAS6, ITGAV and c-Mer) was not affected in *Scarf1*$^{-/-}$ DCs (**Supplementary Fig. 5d**). From these results we concluded that SCARF1 was necessary for the ability of CD8α$^+$ DCs to engulf and clear apoptotic cells *in vivo*.

SCARF1 deficiency results in spontaneous autoimmunity

Defective clearance of apoptotic cells can enhance susceptibility to the autoimmune disease SLE, and autoantigens derived from those apoptotic cells can lead to the production of autoantibodies, a hallmark feature of lupus[34–36]. We hypothesized that the inability of *Scarf1*$^{-/-}$ mice to clear apoptotic cells efficiently would result in spontaneous lupus-associated autoimmune disease. To test our hypothesis, we used an indirect fluorescent antibody assay of antinuclear antibody (ANA) in human epithelial (HEp-2) cells as a sensitive method for detecting antibodies to both RNA- and DNA-containing autoantigens (**Fig. 6a**). Beginning at ~20 weeks of age, a majority (~62%) of the serum from *Scarf1*$^{-/-}$ mice produced a homogenous (~63%) or speckled (~37%) pattern of staining of nuclear ANA (**Fig. 6b**). There was a significantly higher prevalence of ANA$^+$ serum from female *Scarf1*$^{-/-}$ mice (17 of 22; ~77%) than from male *Scarf1*$^{-/-}$ mice (11 of 25; ~48%; **Fig. 6c**). Indeed, there is a strong gender bias in human SLE and in various animal models of lupus in which females are more susceptible to disease[37,38]. Sex hormones and other genetic effects conferred by the female background may be involved in the generation of higher concentrations of systemic autoantibodies than those in male SCARF1-deficient mice[11]. In contrast, none of the serum from their *Scarf1*$^{+/+}$ littermates (control mice) produced any type of staining (**Fig. 6a**), which indicated an absence of nuclear autoantibodies. The homogenous staining pattern in the majority of ANA$^+$ serum from *Scarf1*$^{-/-}$ mice indicated autoantibodies to nucleoproteins and DNA, which have been reported to correlate with the clinical diagnosis of SLE. Autoantibodies with speckled staining patterns are also present in SLE and other disorders, notably Sjogren's syndrome. However, the specificity of the autoantibodies that produce the speckled pattern is less well defined but is often indicative of the presence of autoantibodies to the RNA-containing antigen Smith (SmRNP) and/or to the nuclear protein La. To further define the autoantibody profile,

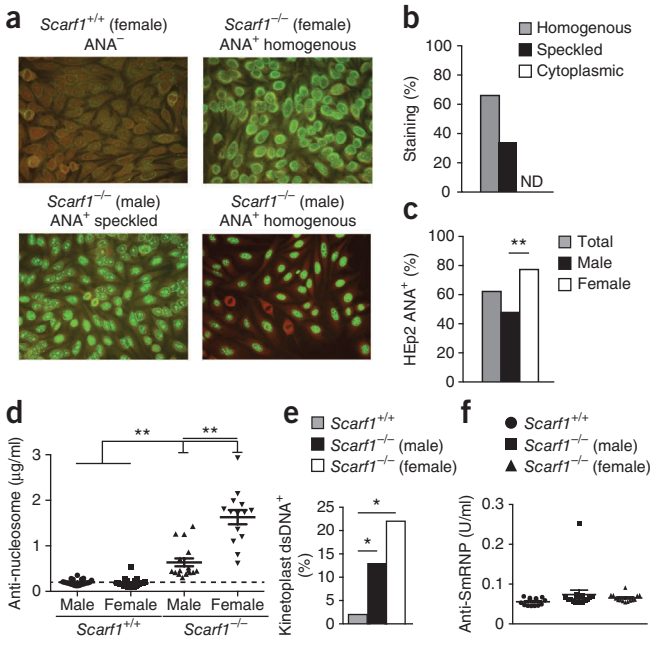

Figure 6 Generation of autoantibodies by *Scarf1*$^{-/-}$ mice. (**a**) ANA immunofluorescence of HEp-2 cells, with serum from 20-week-old *Scarf1*$^{+/+}$ and *Scarf1*$^{-/-}$ mice ($n = 25$ male and 25 female mice per group). Original magnification, ×40. (**b**) Frequency of serum ANA with a nuclear homogenous, nuclear speckled or cytoplasmic staining pattern. ND, not detected. (**c**) Frequency of *Scarf1*$^{-/-}$ mice with positive staining (>1:320 dilution) for ANA. (**d**) ELISA of autoantibodies to nucleosomes (dsDNA-histone) in serum from male and female *Scarf1*$^{+/+}$ and *Scarf1*$^{-/-}$ mice ($n = 14$ per group). (**e**) *C. luciliae* immunofluorescence with serum from male and female *Scarf1*$^{-/-}$ mice ($n = 14$ per group), at a dilution of 1:80. (**f**) ELISA of autoantibodies to SmRNP in serum from male and female *Scarf1*$^{+/+}$ and *Scarf1*$^{-/-}$ mice ($n = 14$ per group). Each symbol (**d**,**f**) represents an individual mouse; small horizontal lines indicate the median (± s.d.). $^{*}P < 0.001$ and $^{**}P < 0.0001$ (Student's *t*-test (**c**,**e**) or Mann-Whitney test (**d**)). Data are representative of at least two experiments.

we used ELISA to quantify the higher concentration of autoantibodies to DNA-containing antigens in *Scarf1*$^{-/-}$ serum. ELISA of autoantibodies to nucleosomes, in which the detection antigen was a combination of histones and double-stranded DNA (dsDNA), showed significantly higher concentration of autoantibodies specific for DNA-histone in *Scarf1*$^{-/-}$ mice than in *Scarf1*$^{+/+}$ mice (**Fig. 6d**). Consistent with the data obtained for ANA, female *Scarf1*$^{-/-}$ mice generated significantly higher concentrations of autoantibodies to nucleosomes than did their male counterparts (**Fig. 6d**). To determine if autoantibodies specific to dsDNA were present, we did the highly specific *Crithida luciliae* immunofluorescence assay. Male (13%) and female (22%) *Scarf1*$^{-/-}$ mice had lower (but readily detectable) concentrations of anti-dsDNA autoantibodies in their serum than did *Scarf1*$^{+/+}$ mice (**Fig. 6e**). Together these data indicated that autoantibodies in *Scarf1*$^{-/-}$ mice 'preferentially' bound to DNA-histone epitopes rather than to non-chromatin DNA, which suggested that chromatin was the physiologically relevant autoantigen. We also quantified autoantibodies to SmRNP and La. Unlike our detection of antibodies to DNA-containing antigens, we did not detect the presence of serum antibodies to SmRNP or La (**Fig. 6f** and data not shown); thus, the autoantigen responsible for the speckled ANA pattern noted in ~23% of *Scarf1*$^{-/-}$ mice remains to be identified.

Spontaneous inflammation in *Scarf1*$^{-/-}$ mice

Because we had observed a significant effect of SCARF1 deficiency on autoantibody production, we next determined whether the absence of this receptor had a significant effect on other clinical manifestations

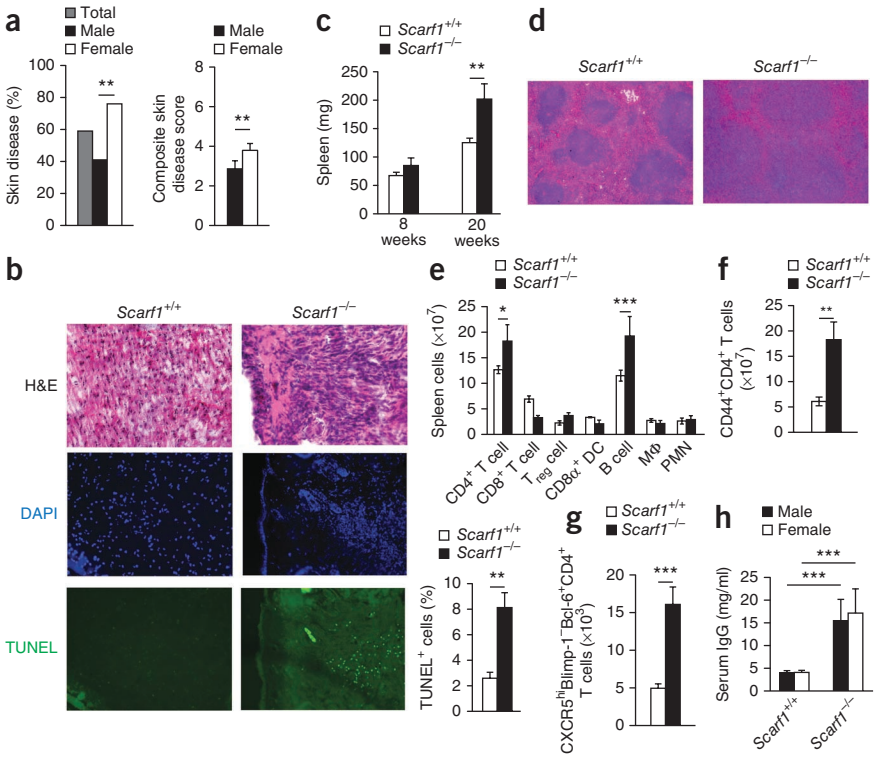

Figure 7 Enhanced immunological activation in *Scarf1*$^{-/-}$ mice. (**a**) Incidence and severity of skin disease in *Scarf1*$^{-/-}$ mice ($n = 47$ total: 22 female and 25 male). (**b**) Fluorescence microscopy (left) of cryosections of skin from 20-week-old female *Scarf1*$^{+/+}$ and *Scarf1*$^{-/-}$ mice, stained with hematoxylin and eosin (H&E), and with the nuclear stain DAPI (blue) and by TUNEL (green) for the detection of apoptotic cells, and quantification of images at left ($n = 8$ mice per group) by automated analysis of DAPI-TUNEL staining (right). Original magnification (left), ×20. (**c**) Weight of spleens from *Scarf1*$^{+/+}$ and *Scarf1*$^{-/-}$ mice ($n = 8$ per group) at 8 and 20 weeks of age. (**d**) Hematoxylin-and-eosin staining of cryosections of spleens from *Scarf1*$^{+/+}$ and *Scarf1*$^{-/-}$ mice ($n = 6$ per group). Original magnification, ×10. (**e**) Absolute number of cells of the immune system (horizontal axis) in spleens from *Scarf1*$^{+/+}$ and *Scarf1*$^{-/-}$ mice ($n = 6$ per group), determined by staining of surface markers and flow cytometry. (**f**,**g**) Absolute number of $CD44^{+}CD4^{+}$ activated T cells (**f**) and $CXCR5^{hi}Blimp\text{-}1^{-}Bcl\text{-}6^{+}CD4^{+}$ follicular helper T cells (**g**) in spleens from *Scarf1*$^{+/+}$ and *Scarf1*$^{-/-}$ mice ($n = 6$ per group). (**h**) Concentration of total IgG in serum from 20-week old male and female *Scarf1*$^{+/+}$ and *Scarf1*$^{-/-}$ mice ($n = 12$ per group). $^{*}P < 0.05$, $^{**}P < 0.01$ and $^{***}P < 0.001$ (Student's *t*-test). Data are representative of at least three experiments (**a**–**c**,**e**–**h**; mean and s.d.) or two experiments (**d**).

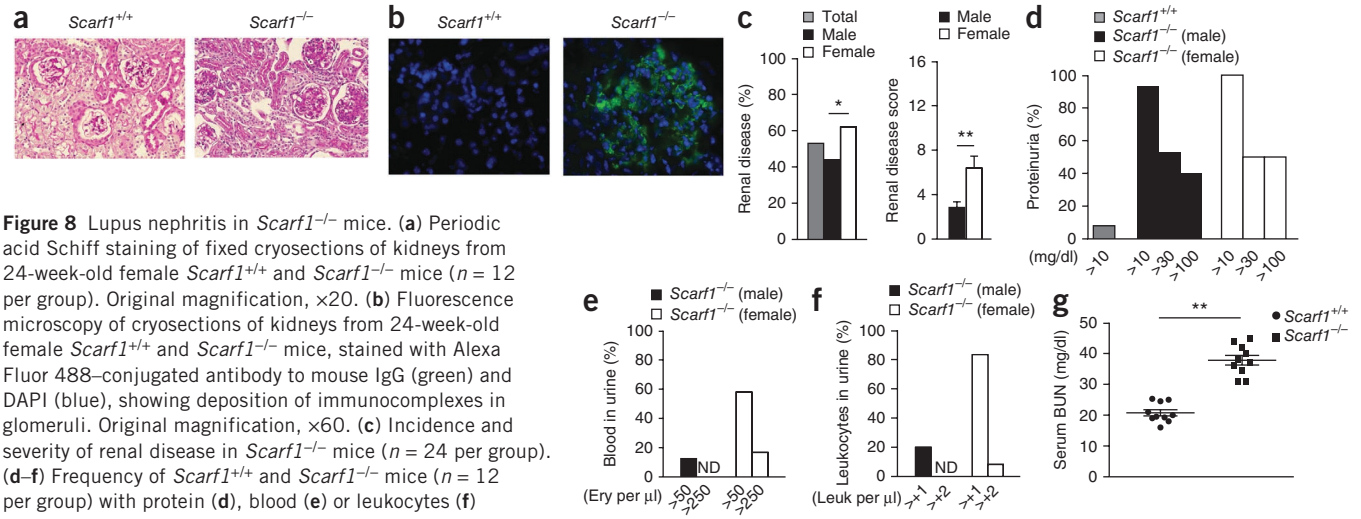

Figure 8 Lupus nephritis in *Scarf1*$^{-/-}$ mice. (**a**) Periodic acid Schiff staining of fixed cryosections of kidneys from 24-week-old female *Scarf1*$^{+/+}$ and *Scarf1*$^{-/-}$ mice ($n = 12$ per group). Original magnification, ×20. (**b**) Fluorescence microscopy of cryosections of kidneys from 24-week-old female *Scarf1*$^{+/+}$ and *Scarf1*$^{-/-}$ mice, stained with Alexa Fluor 488–conjugated antibody to mouse IgG (green) and DAPI (blue), showing deposition of immunocomplexes in glomeruli. Original magnification, ×60. (**c**) Incidence and severity of renal disease in *Scarf1*$^{-/-}$ mice ($n = 24$ per group). (**d**–**f**) Frequency of *Scarf1*$^{+/+}$ and *Scarf1*$^{-/-}$ mice ($n = 12$ per group) with protein (**d**), blood (**e**) or leukocytes (**f**) in the urine, assessed in a metabolic chamber for 24 h. Ery, erythrocyte. (**g**) Blood urea nitrogen (BUN) in *Scarf1*$^{+/+}$ and *Scarf1*$^{-/-}$ mice. Each symbol represents an individual mouse ($n = 10$ per genotype); small horizontal lines indicate the mean (and s.d.) of at least triplicates. $^{*}P < 0.01$ and $^{**}P < 0.001$ (Student's *t*-test). Data are representative of at least three independent experiments (error bars (**c**), s.d.).

of lupus-like autoimmune disease. *Scarf1*$^{-/-}$ mice also had a significantly greater incidence and severity of skin disease, which was not present in wild-type mice (**Fig. 7a**). Beginning at ~20 weeks of age, most *Scarf1*$^{-/-}$ mice developed skin inflammation on their back, head and face, which was often accompanied by hair loss and whisker loss. Female *Scarf1*$^{-/-}$ mice were more susceptible to skin disease than were their male counterparts. Cryosections of skin lesions from 20-week-old *Scarf1*$^{-/-}$ female mice showed cellular infiltration and the presence of apoptotic cells (**Fig. 7b**). In addition, we observed more splenomegaly in *Scarf1*$^{-/-}$ mice over 20 weeks of age than in their age-matched wild-type littermates (**Fig. 7c**). Cryosection of spleens from *Scarf1*$^{-/-}$ mice demonstrated they had larger germinal centers than did those of *Scarf1*$^{+/+}$ mice (**Fig. 7d**). *Scarf1*$^{-/-}$ mice had significantly more CD4^{+} T cells and B cells in the spleen (**Fig. 7e**). The greater weight of *Scarf1*$^{-/-}$ spleens was accompanied by the accumulation of lymphocytes with an activated phenotype. *Scarf1*$^{-/-}$ mice had significantly more activated CD44^{+}CD4^{+} T cells and CXCR5^{+}Blimp-1^{-} Bcl-6^{+}CD4^{+} follicular helper T cells than did their wild-type counterparts (**Fig. 7f,g**). As a measure of global B cell activation, we quantified total immunoglobulin G (IgG) in the serum. *Scarf1*$^{-/-}$ mice had significantly higher concentrations of total serum IgG than *Scarf1*$^{+/+}$ mice, and this result was independent of the sex of the mice (**Fig. 7h**). Together these data demonstrated that the genetic absence of *Scarf1* led to spontaneous autoimmune disease activity and global activation of cells of the immune system.

Nephritis in *Scarf1*$^{-/-}$ mice

One of the important end-organ pathologies in lupus is nephritis. In agreement with other evidence of enhanced disease activity, *Scarf1*$^{-/-}$ mice developed kidney disease. We observed greater glomerular size, cellularity and deposition of protein in periodic acid Schiff–stained kidney sections from *Scarf1*$^{-/-}$ mice than in their *Scarf1*$^{+/+}$ counterparts (**Fig. 8a**). One of the main clinical pathogenic outcomes of circulating autoantibodies in lupus is their deposition as immunocomplexes in the kidney, which leads to glomerulonephritis[39]. Examination of kidney cryosections showed considerable deposition of IgG immunocomplexes in the glomeruli of *Scarf1*$^{-/-}$ mice (**Fig. 8b**). Meanwhile, female *Scarf1*$^{-/-}$ mice had a significantly higher incidence and severity of renal disease than did male *Scarf1*$^{-/-}$ mice (**Fig. 8c**).

Consistent with that kidney disease, we found, by 24-hour quantitative urine collection, that >90% of *Scarf1*$^{-/-}$ mice had at least moderate proteinuria (**Fig. 8d**). Moreover, most female *Scarf1*$^{-/-}$ mice also had pyuria and hematuria (**Fig. 8e,f**). As another measure of kidney function, we also found that *Scarf1*$^{-/-}$ mice had a significantly higher concentration of blood urea nitrogen than did *Scarf1*$^{+/+}$ mice (**Fig. 8g**), indicative of ongoing kidney disease in the mutant mice. There was no statistically significant difference between male and female *Scarf1*$^{-/-}$ mice or between *Scarf1*$^{+/+}$ mice and *Scarf1*$^{-/-}$ mice in survival for up to 1 year (data not shown), which suggested that other pathways were able to partially compensate for *Scarf1* deficiency and thereby allow these mice to tolerate this chronic autoimmune disease.

DISCUSSION

The data presented here have filled several gaps in the understanding of the clearance of apoptotic cells and regulation of autoimmunity. Here we have presented experimental evidence that SCARF1 is a receptor that is critical for the recognition and capture of apoptotic cells via binding to C1q that is adhered to newly exposed phosphatidylserine on the surface of the apoptotic cells, a process that is necessary for the prevention of lupus-like disease. That conclusion was based on the following: SCARF1 recognized and engulfed apoptotic cells at early stages of apoptosis before the loss of membrane integrity, a process critical for maintaining immunotolerance; the binding of SCARF1 to apoptotic cells and its uptake of those cells required exposure of C1q and phosphatidylserine on dying cells; evidence obtained by dot blot analysis, ELISA and measurement of surface plasmon resonance showed that SCARF1 recognized C1q specifically and avidly ($K_d = 1.24 \times 10^{-7}$ M); SCARF1-deficient mice accumulated apoptotic and necrotic cells in their blood and tissues; and SCARF1-deficient mice spontaneously developed clinical manifestations of lupus disease, including the generation of autoantibodies to chromatin, activation of cells of the immune system, skin inflammation and kidney disease (exemplified by the deposition of immunocomplexes in glomeruli, along with proteinuria). Together these data demonstrated an important role for SCARF1 in the removal of apoptotic cells *in vitro* and that its absence *in vivo* resulted in the spontaneous development of autoimmune disease.

The pathways that mediate engulfment of dying cells are conserved across evolution. In the worm, two partially redundant pathways exist

for the removal of 'corpses', with ced-1, ced-6 and ced-7 functioning in one pathway, and ced-2, ced-5, ced-10 and ced-12 functioning in the other[40]. In *Drosophila*, dead cells are engulfed by macrophages that express Draper, a receptor that is structurally and functionally similar to CED-1 (refs. 41,42). In mammals, five proteins (MEGF10, MEGF11, Jedi-1, SCARF1 and CD91) have been identified that share homology with CED-1 and Draper[29,43]. The expression of MEGF10 or Jedi-1 by glial cells has been shown to confer the ability to bind and engulf apoptotic neurons *in vitro*[44,45]. However, a transgene encoding MEGF10 failed to 'rescue' the engulfment defect in CED-1-deficient worms, the ligands on apoptotic cells recognized by MEGF10 and Jedi-1 are not known, and mice deficient in these receptors that could be used to confirm those findings have not yet to been generated. The interaction of CD91 with apoptotic cells has been shown to occur through binding to calreticulin adherent to the surface of the apoptotic cells by C1q and/or phosphatidylserine[46]. Loss of CD91 impairs the uptake of apoptotic cells *in vitro*, but its role *in vivo* has not been determined, as CD91-deficient mice die early during gestation. CED-1 and SCARF1 share an evolutionarily conserved function in the recognition of and host defense against pathogenic fungi[27]. Here we found that SCARF1 also shares with CED-1 an evolutionarily conserved function in the capture of apoptotic cells. Furthermore, SCARF1 is the first C1q receptor, to our knowledge, that has been shown to be necessary for removal of apoptotic cells *in vivo*. Moreover, the susceptibility to and severity of the spontaneous autoimmune disease of SCARF1-deficient mice is similar to that of C1q-deficient mice[47].

Many receptors and soluble bridging molecules have been linked to the clearance of apoptotic cells, and mice deficient in C1q, MFG-E8, TIM4 or c-Mer develop spontaneous autoimmune disease depending on their genetic background[10,18,47–49]. CD91 and calreticulin have also been shown to be involved in the uptake of apoptotic cells *in vitro*; however, their role *in vivo* remains unclear, as mice deficient in calreticulin or CD91 die *in utero*, which suggests that these pathways be important during development. Our *in vitro* and *in vivo* data demonstrated that the SCARF1 pathway for clearance of apoptotic cells was not completely nonredundant but contributed ~40–70% to the capture of apoptotic cells, depending on the type of phagocytic cell. These data indicated that other pathways for the clearance of apoptotic cells, such as phosphatidylserine–MFG-E8–integrins $\alpha_v\beta_3$ and β_5, phosphatidylserine-calreticulin-CD91, and/or phosphatidylserine–TIM-3–TIM-4 probably contributed to the other 30–60%. Indeed, published studies have indicated that macrophages deficient in MFG-E8, calreticulin or C1q have ~75%, ~60% or ~50% less capture of apoptotic cells, respectively[10,16,18,46]. This growing body of evidence, including our findings described here, suggests that all of these receptors partially contribute to the clearance of apoptotic cells, which may represent a new collective paradigm with which to explain clearance of apoptotic cells *in vivo* that has not been recognized, to our knowledge, before our work here. This hypothesis has been tested by studies showing that double deficiency in TIM4 and MFG-E8 results in a more deleterious phenotype than does single deficiency in either[50]. Similarly, we hypothesize that double deficiency in SCARF1 and MFG-E8 or in SCARF1 and TIM4 would result in a more deleterious phenotype than would single deficiency in any of those alone. For full understanding of the relative contribution of each molecule to clearance of apoptotic cells, future studies will need to generate such doubly deficient mice.

Collectively, these data indicate that the immune system has developed a fail-safe mechanism involving several receptors and bridging proteins expressed by different cell types and in specific organs for the removal of dying cells to maintain tolerance and prevent autoimmunity. The identification of the main molecules and receptors and how they function to internalize and process apoptotic debris could lead to therapeutic exploitation not only for the removal of unwanted cells but as an immunosuppressive or anti-inflammatory strategy. As in human patients, the lupus phenotype of SCARF1-deficient mice was more prevalent and severe in females, which indicates that SCARF1-deficient mice may be useful as a new model of spontaneous lupus for the study of human lupus that can be used to provide better understanding of the mechanisms used for the clearance of apoptotic cells in healthy and diseased states to identify targets for new therapeutic strategies.

METHODS

Methods and any associated references are available in the online version of the paper.

Note: Any Supplementary Information and Source Data files are available in the online version of the paper.

ACKNOWLEDGMENTS

We thank Y.F. Peng (University of Washington) for *Mfge8*$^{-/-}$ mice; M. Michalak (University of Alberta) for K41 (calreticulin-sufficient) and K42 (calreticulin-deficient) MEFs; and M.J. Shlomchik and P. Mundel and members of their laboratories for technical assistance and discussions. Supported by the National Institute of Allergy and Infectious Diseases (R01-AI084884 to T.K.M.; U24 AI082660 to J.E.K.; and T32-AI007061 to Z.G.R.-O.), the National Institute of Arthritis, Musculoskeletal and Skin Diseases (K01-AR051367 to T.K.M.), the National Institute of Diabetes and Digestive and Kidney Diseases (F32-DK097891 to W.F.P.), the Lupus Research Institute (T.K.M. and N.H.), the Alliance for Lupus Research (T.K.M. and N.H.) and the American Society of Nephrology (W.F.P.).

AUTHOR CONTRIBUTIONS

T.K.M., Z.G.R.-O. and W.F.P. planned the research, analyzed and interpreted data and wrote the manuscript; Z.G.R.-O. did most of the experiments; C.J.B. helped with mouse breeding and genotyping; W.F.P., A.P. and T.I. did and analyzed ELISA, PCR and mouse-pathology studies; N.H. and A.D.L. analyzed and interpreted data; T.K.M., J.E.K., and M.H.B. contributed to the generation of SCARF1-deficient mice; and all authors participated in editing the manuscript.

COMPETING FINANCIAL INTERESTS

The authors declare no competing financial interests.

1. Elliott, M.R. & Ravichandran, K.S. Clearance of apoptotic cells: implications in health and disease. *J. Cell Biol.* **189**, 1059–1070 (2010).
2. Devitt, A. & Marshall, L.J. The innate immune system and the clearance of apoptotic cells. *J. Leukoc. Biol.* **90**, 447–457 (2011).
3. Lauber, K., Blumenthal, S.G., Waibel, M. & Wesselborg, S. Clearance of apoptotic cells: getting rid of the corpses. *Mol. Cell* **14**, 277–287 (2004).
4. Erwig, L.P. & Henson, P.M. Clearance of apoptotic cells by phagocytes. *Cell Death Differ.* **15**, 243–250 (2008).
5. Munoz, L.E. *et al.* Apoptosis in the pathogenesis of systemic lupus erythematosus. *Lupus* **17**, 371–375 (2008).
6. Ravichandran, K.S. & Lorenz, U. Engulfment of apoptotic cells: signals for a good meal. *Nat. Rev. Immunol.* **7**, 964–974 (2007).
7. Nagata, S., Hanayama, R. & Kawane, K. Autoimmunity and the clearance of dead cells. *Cell* **140**, 619–630 (2010).
8. Shao, W.H. & Cohen, P.L. Disturbances of apoptotic cell clearance in systemic lupus erythematosus. *Arthritis Res. Ther.* **13**, 202 (2011).
9. Fadok, V.A. *et al.* Exposure of phosphatidylserine on the surface of apoptotic lymphocytes triggers specific recognition and removal by macrophages. *J. Immunol.* **148**, 2207–2216 (1992).
10. Kobayashi, N. *et al.* TIM-1 and TIM-4 glycoproteins bind phosphatidylserine and mediate uptake of apoptotic cells. *Immunity* **27**, 927–940 (2007).
11. Park, D. *et al.* BAI1 is an engulfment receptor for apoptotic cells upstream of the ELMO/Dock180/Rac module. *Nature* **450**, 430–434 (2007).
12. Hanayama, R. *et al.* Identification of a factor that links apoptotic cells to phagocytes. *Nature* **417**, 182–187 (2002).

13. Païdassi, H. *et al.* C1q binds phosphatidylserine and likely acts as a multiligand-bridging molecule in apoptotic cell recognition. *J. Immunol.* **180**, 2329–2338 (2008).
14. Païdassi, H. *et al.* Investigations on the C1q-calreticulin-phosphatidylserine interactions yield new insights into apoptotic cell recognition. *J. Mol. Biol.* **408**, 277–290 (2011).
15. Galvan, M.D., Greenlee-Wacker, M.C. & Bohlson, S.S. C1q and phagocytosis: the perfect complement to a good meal. *J. Leukoc. Biol.* **92**, 489–497 (2012).
16. Gardai, S.J. *et al.* Cell-surface calreticulin initiates clearance of viable or apoptotic cells through trans-activation of LRP on the phagocyte. *Cell* **123**, 321–334 (2005).
17. Manderson, A.P., Botto, M. & Walport, M.J. The role of complement in the development of systemic lupus erythematosus. *Annu. Rev. Immunol.* **22**, 431–456 (2004).
18. Hanayama, R. *et al.* Autoimmune disease and impaired uptake of apoptotic cells in MFG-E8-deficient mice. *Science* **304**, 1147–1150 (2004).
19. Taylor, P.R. *et al.* A hierarchical role for classical pathway complement proteins in the clearance of apoptotic cells *in vivo*. *J. Exp. Med.* **192**, 359–366 (2000).
20. Mukhopadhyay, S., Pluddemann, A. & Gordon, S. Macrophage pattern recognition receptors in immunity, homeostasis and self tolerance. *Adv. Exp. Med. Biol.* **653**, 1–14 (2009).
21. Adachi, H., Tsujimoto, M., Arai, H. & Inoue, K. Expression cloning of a novel scavenger receptor from human endothelial cells. *J. Biol. Chem.* **272**, 31217–31220 (1997).
22. Tamura, Y. *et al.* Scavenger receptor expressed by endothelial cells I (SREC-I) mediates the uptake of acetylated low density lipoproteins by macrophages stimulated with lipopolysaccharide. *J. Biol. Chem.* **279**, 30938–30944 (2004).
23. Berwin, B., Delneste, Y., Lovingood, R.V., Post, S.R. & Pizzo, S.V. SREC-I, a type F scavenger receptor, is an endocytic receptor for calreticulin. *J. Biol. Chem.* **279**, 51250–51257 (2004).
24. Jeannin, P. *et al.* Complexity and complementarity of outer membrane protein A recognition by cellular and humoral innate immunity receptors. *Immunity* **22**, 551–560 (2005).
25. Hölzl, M.A. *et al.* The zymogen granule protein 2 (GP2) binds to scavenger receptor expressed on endothelial cells I (SREC-I). *Cell. Immunol.* **267**, 88–93 (2011).
26. Murshid, A., Gong, J. & Calderwood, S.K. Heat shock protein 90 mediates efficient antigen cross presentation through the scavenger receptor expressed by endothelial cells-I. *J. Immunol.* **185**, 2903–2917 (2010).
27. Means, T.K. *et al.* Evolutionarily conserved recognition and innate immunity to fungal pathogens by the scavenger receptors SCARF1 and CD36. *J. Exp. Med.* **206**, 637–653 (2009).
28. Rechner, C., Kuhlewein, C., Muller, A., Schild, H. & Rudel, T. Host glycoprotein Gp96 and scavenger receptor SREC interact with PorB of disseminating *Neisseria gonorrhoeae* in an epithelial invasion pathway. *Cell Host Microbe* **2**, 393–403 (2007).
29. Zhou, Z., Hartwieg, E. & Horvitz, H.R. CED-1 is a transmembrane receptor that mediates cell corpse engulfment in *C. elegans*. *Cell* **104**, 43–56 (2001).
30. Means, T.K. Fungal pathogen recognition by scavenger receptors in nematodes and mammals. *Virulence* **1**, 37–41 (2010).
31. Ishii, J. *et al.* SREC-II, a new member of the scavenger receptor type F family, trans-interacts with SREC-I through its extracellular domain. *J. Biol. Chem.* **277**, 39696–39702 (2002).
32. Yoshiizumi, K., Nakajima, F., Dobashi, R., Nishimura, N. & Ikeda, S. Studies on scavenger receptor inhibitors. Part 1: synthesis and structure-activity relationships of novel derivatives of sulfatides. *Bioorg. Med. Chem.* **10**, 2445–2460 (2002).
33. Iyoda, T. *et al.* The CD8+ dendritic cell subset selectively endocytoses dying cells in culture and *in vivo*. *J. Exp. Med.* **195**, 1289–1302 (2002).
34. Tan, E.M. *et al.* The 1982 revised criteria for the classification of systemic lupus erythematosus. *Arthritis Rheum.* **25**, 1271–1277 (1982).
35. Tsokos, G.C. Systemic lupus erythematosus. *N. Engl. J. Med.* **365**, 2110–2121 (2011).
36. Casciola-Rosen, L.A., Anhalt, G. & Rosen, A. Autoantigens targeted in systemic lupus erythematosus are clustered in two populations of surface structures on apoptotic keratinocytes. *J. Exp. Med.* **179**, 1317–1330 (1994).
37. Zandman-Goddard, G., Peeva, E. & Shoenfeld, Y. Gender and autoimmunity. *Autoimmun. Rev.* **6**, 366–372 (2007).
38. Xu, Y. *et al.* Pleiotropic IFN-dependent and -independent effects of IRF5 on the pathogenesis of experimental lupus. *J. Immunol.* **188**, 4113–4121 (2012).
39. Winfield, J.B., Faiferman, I. & Koffler, D. Avidity of anti-DNA antibodies in serum and IgG glomerular eluates from patients with systemic lupus erythematosus. Association of high avidity antinative DNA antibody with glomerulonephritis. *J. Clin. Invest.* **59**, 90–96 (1977).
40. Reddien, P.W., Cameron, S. & Horvitz, H.R. Phagocytosis promotes programmed cell death in *C. elegans*. *Nature* **412**, 198–202 (2001).
41. Awasaki, T. *et al.* Essential role of the apoptotic cell engulfment genes draper and ced-6 in programmed axon pruning during *Drosophila* metamorphosis. *Neuron* **50**, 855–867 (2006).
42. Hamon, Y. *et al.* Cooperation between engulfment receptors: the case of ABCA1 and MEGF10. *PLoS ONE* **1**, e120 (2006).
43. Su, H.P. *et al.* Interaction of CED-6/GULP, an adapter protein involved in engulfment of apoptotic cells with CED-1 and CD91/low density lipoprotein receptor-related protein (LRP). *J. Biol. Chem.* **277**, 11772–11779 (2002).
44. Wu, H.H. *et al.* Glial precursors clear sensory neuron corpses during development via Jedi-1, an engulfment receptor. *Nat. Neurosci.* **12**, 1534–1541 (2009).
45. Scheib, J.L., Sullivan, C.S. & Carter, B.D. Jedi-1 and MEGF10 signal engulfment of apoptotic neurons through the tyrosine kinase Syk. *J. Neurosci.* **32**, 13022–13031 (2012).
46. Ogden, C.A. *et al.* C1q and mannose binding lectin engagement of cell surface calreticulin and CD91 initiates macropinocytosis and uptake of apoptotic cells. *J. Exp. Med.* **194**, 781–795 (2001).
47. Botto, M. *et al.* Homozygous C1q deficiency causes glomerulonephritis associated with multiple apoptotic bodies. *Nat. Genet.* **19**, 56–59 (1998).
48. Wong, K. *et al.* Phosphatidylserine receptor Tim-4 is essential for the maintenance of the homeostatic state of resident peritoneal macrophages. *Proc. Natl. Acad. Sci. USA* **107**, 8712–8717 (2010).
49. Cohen, P.L. *et al.* Delayed apoptotic cell clearance and lupus-like autoimmunity in mice lacking the c-mer membrane tyrosine kinase. *J. Exp. Med.* **196**, 135–140 (2002).
50. Miyanishi, M., Segawa, K. & Nagata, S. Synergistic effect of Tim4 and MFG-E8 null mutations on the development of autoimmunity. *Int. Immunol.* **24**, 551–559 (2012).

ONLINE METHODS

Reagents. Reagents were from Sigma-Aldrich unless stated otherwise. Complete medium consisted of RPMI-1640 medium (Invitrogen) or DMEM (Invitrogen) supplemented with 100 U/ml penicillin, 100 U/ml streptomycin, 2 mM L-glutamine and 10% FCS. The HEK293T cell line (HCL4517) was from Fisher Scientific, and MEFs (SCRC-1008) were from American Type Culture Collection. All cell lines were free of mycoplasma, as determined by a Mycoplasma Detection PCR Kit (Sigma-Aldrich). Human anti-SCARF1 was from R&D Systems (monoclonal mouse IgG2B; 373606) and mouse anti-SCARF1 was from Proteintech (rabbit polyclonal; 13702-1-AP). All other antibodies were from eBioscience, unless otherwise specified.

Mice. All mice were maintained under microisolation in specific pathogen–free conditions at the animal facility of Massachusetts General Hospital under a protocol approved by the Institutional Animal Care and Use Committee. Wild-type C57BL/6 mice were from The Jackson Laboratories. To generate *Scarf1*$^{-/-}$ mice, we constructed a targeting vector that contained 4.42 kilobases of 5′ sequence upstream of the transcriptional start site, a neomycin-resistance cassette that replaced exons 1–8 (which encode the entire extracellular and transmembrane domains), and 1.85 kilobases of 3′ sequence spanning exons 9–10. The primers used to amplify the 5′ long arm and the 3′ short arm were as follows: 5′ long arm forward (5Arm Fw1), 5′-CCCAGTCCTCCTGGAACTACAACTT-3′, and reverse (5Arm Rv1), 5′-CCACAGGTCCCTGAAACACTAGAGA-3′; and 3′ short arm forward (3Arm Fw1), 5′-AAGAAAAGTGAAATCAGAGCCGACA-3′, and reverse (3Arm Rv1), 5′-CCAAAACACCATTACTACTGCCGAA-3′. Those genomic regions were ligated into the targeting vector OSDupDel.Neo (Open Biosystems). The linearized vector was transfected into C57BL/6 ES cells by electroporation by the inGenious Targeting Laboratory, and targeted clones that were selected in the presence of the antibiotic neomycin were identified by PCR and Southern blot analysis. Targeted embryonic stem cell clones were injected into C57BL/6 mice blastocysts, which yielded several lines of chimeric mice that transmitted the disrupted allele through germline DNA. Offspring of *Scarf1*$^{-/-}$ mice were produced at normal Mendelian ratios. Mice were not randomized or placed in specific groups for these studies.

Genotyping and Southern blot analysis of *Scarf1*. Homologous recombination in electroporated embryonic stem cell clones or genomic DNA obtained from tail tissue was assessed by PCR and Southern blot analysis. PCR primer pairs were as follows: wild-type forward (WT Fw1), 5′-AGCCTGGAACTGCATGTCTT-3′, and reverse (WT Rv1), 5′-TGAATGCCTTACAGCACAGC-3′; and *Scarf1*$^{-/-}$ forward (KO Fw1), 5′-CTTCTATCGCCTTCTTGACGAGT-3′, and reverse (KO Rv1), 5′-TAGATACCTCTCCTTCGCTCT-3′. The probe (326–base pair) and primer pairs for Southern blot analysis were South Fw1 (forward), 5′-CAAGATGTCACCACTCATGCCAAAA-3′, and South Rv1 (reverse), 5′-ACAGGAGCATCTGAACCCTCTCGTA-3′. For screening by Southern blot analysis, genomic DNA was digested with BamHI before separation by electrophoresis through a gel. The DNA was transferred to nitrocellulose and incubated with a radiolabeled probe. The digestion pattern was a wild-type band at 5,110 base pairs and a 'gene-targeted' band at 6,122 base pairs.

Generation of apoptotic cells. Mouse primary B cells were isolated by negative selection from the spleen with an EasySep Mouse B Cell enrichment kit according to the manufacturer's instructions (STEMCELL Technologies). Apoptotic cells were generated from primary B cells, HEK293T cells and MEFs according to the method described below. For all assays, unless specified otherwise, apoptotic cells were labeled with CFSE (carboxyfluorescein diacetate succinimidyl ester) or pHrodo (Invitrogen).

For the generation of apoptotic cells by osmotic shock, cells were first centrifuged at 800*g* for 5 min. Cells were then washed once with PBS and resuspended for 10 min in hypertonic media (DMEM supplemented with 10% (wt/vol) polyethylene glycol 1000, 0.5 M sucrose, 10 mM HEPES, pH 7.2). Immediately afterward, 30 ml of hypotonic medium (60% DMEM and 40% water) was added, followed by incubation for 5 min. Cells were then washed and resuspended in complete DMEM, followed by culture for 3 h at 37 °C. The generation of apoptotic cells by ultraviolet radiation was done by placement of a flask of cells into a ultraviolet transilluminator set to 100 Joules/m^2, followed by culture for 3 h. The generation of apoptotic cells by ^{137}Cs irradiation was done by exposure of cells to 3,000 rads. Apoptotic cells were generated from *Mfge8*$^{-/-}$ mice (a gift from Y.F. Peng) and from K41 (calreticulin-sufficient) and K42 (calreticulin-deficient) MEFs (a gift from M. Michalak). Cells were used when most cells were apoptotic, as defined by annexin V–positive and propidium iodide–negative staining by flow cytometry.

Generation of liposomes. Small unilamellar vesicles (liposomes) were prepared as described[9]. Pure phospholipids were sonicated and specific phospholipids were prepared in sodium phosphate buffer by extrusion at 37 °C through a 0.1-μm polycarbonate filter with a mini-extruder set (Avanti polar lipids). Liposomes were composed of 100% mol phosphatidylcholine or a mixture of 70% mol phosphatidylcholine and 30% mol phosphatidylserine.

Dot-blot and binding assays. Membrane lipid strips (Echelon Bioscience) were spotted with ten membrane lipids (100 pmol each). Nonspecific binding of membranes were blocked by incubation for 1 h with 3% BSA in TBS-T (50 mM Tris, 0.5 M NaCl and 0.05% Tween-20, pH 7.4). After that blockade, membranes were incubated for 1 h with soluble recombinant SCARF1 protein (R&D Systems), then were washed and incubated with anti-SCARF1 (mouse; 373606; R&D Systems), followed by incubation for 1 h with a horseradish peroxidase–labeled secondary antibody (goat; HAF007; R&D Systems). Binding was detected by chemiluminescent detection. ELISA was used to confirm the interaction of SCARF1 with other markers of apoptotic cells. PVC microtiter plates were coated overnight at 4 °C with acLDL, C1q, BSA, phosphatidylserine, phosphatidylcholine or calreticulin. Plates were washed and nonspecific binding was blocked, followed by incubation with SCARF1 protein and then primary antibodies (mouse; 373606; R&D Systems) and horseradish peroxidase–conjugated secondary antibodies (goat; HAF007; R&D Systems). Absorbance at 450 nm was measured with a plate reader (Molecular Devices) and Softmax Pro software. Binding was measured according to the assay manufacturer's instructions (Biacore). C1q, phosphatidylserine and calreticulin were immobilized on a CM5 sensor chip, and the binding affinity of SCARF1 was measured with Biacore 3000 system and software (GE Healthcare).

Nucleofection. A Nucleofector kit for Primary Mammalian Endothelial Cells was used for the transfection of endothelial cells, and a Nucleofector kit V was used for the transfection of DCs and macrophages, according to the manufacturer's instructions (Lonza). Primary CD8α$^+$ DCs or macrophages (2×10^6) or endothelial cells (5×10^5) isolated from *Scarf1*$^{+/+}$ and *Scarf1*$^{-/-}$ mice were transfected with a Nucleofector II by the Nucleofector program D-32 or M-002 with 2 μg mammalian expression vector encoding GFP alone (pMAX-GFP; Amaxa) or mouse SCARF1 tagged at the C terminus with GFP. Experiments were done 24 h later, at which time the transfection efficiency was >50% and cell viability was >80%, as determined by staining of GFP and with annexin V and propidium iodide, respectively. For flow cytometry, cells were pregated according to GFP expression for analysis of cells expressing GFP or SCARF1-GFP that captured red dye–labeled apoptotic cells.

Real-time quantitative PCR. Total RNA was extracted with an RNeasy kit and was treated with DNase according to the manufacturer's protocol (Qiagen), and each sample was reverse-transcribed with MultiScribe Reverse Transcriptase (Applied Biosystems). Each 25-μl volume for PCR contained 2 μl cDNA, 12.5 μl 2× SYBR Green Master Mix (Applied Biosystems) and 500 nM sense and antisense primers. Oligonucleotide primer sequences (designed on the PrimerBank website obtained from Integrated DNA Technologies) were as follows: human GAPDH, 5′-GAAGGTGAAGGTCGGAGTC-3′ and 5′-GAAGATGGTGATGGGATTTC-3′; human IL8, 5′-CTGGCCGTGGCTCTCTTG-3′ and 5′-CCTTGGCAAAACTGCACCTT-3′; mouse B2M, 5′-TTCTGGTGCTTGTCTCACTGA-3′ and 5′-CAGTATGTTCGGCTTCCCATTC-3′; LOX-1, 5′-AAGCGAACCTTACTCAGCAGG-3′ and 5′-TGGATTTCTCATTCAGCTTCTGG; MARCO, 5′-CTGTGGCAATGGATCACTAGC-3′ and 5′-CTCCTGGCTGGTATGGACC-3′; SR-A1, 5′-TGAACGAGAGGATGCTGACTG-3′ and 5′-GGAGGGGCCATTTTTAGTGC-3′; CD14, 5′-GCACACTCACTCAACTTTTCCT-3′ and 5′-GCTGAGATCAGTCCTCTCTCG-3′; SCARF1, 5′-AGCCTGGAACTGCATGTCTT-3′ and 5′-TGAATGCC

TTACAGCACAGC-3′; TIM3, 5′-TCAGGTCTTACCCTCAACTGTG-3′ and 5′-GGGCAGATAGGCATTTTTACCA-3′; TIM4, 5′-GTGTACTGCTGCCG TATAGAGG-3′ and 5′-TGGTGGTTGGGAGAACAGATG-3′; TIM1, 5′-ACATA TCGTGGAATCACAACGAC-3′ and 5′-ACAAGCAGAAGATGGGCAT TG-3′; ITGAV, 5′-CCGTGGACTTCTTCGAGCC-3′ and 5′-CTGTTGAATC AAACTCAATGGGC-3′; MFGE8, 5′-AGATGCGGGTATCAGGTGTGA-3′ and 5′-GGGGCTCAGAACATCCGTG-3′; CD91, 5′-ACTATGGATGCCCC TAAAACTTG-3′ and 5′-GCAATCTCTTTCACCGTCACA-3′; GAS6, 5′-TG CTGGCTTCCGAGTCTTC-3′ and 5′-CGGGGTCGTTCTCGAACAC-3′; c-Mer, 5′-ACCCAGTTGCTAGAGAGCTG-3′ and 5′-TGGTGAGTCTGT CTCCGGTAA-3′; and C1q, 5′-AAAGGCAATCCAGGCAATATCA-3′ and 5′-TGGTTCTGGTATGGACTCTCC-3′. The fluorescence emitted for each reaction was measured three times during the annealing-extension phase, and amplification plots were analyzed with MX4000 software, version 3.0 (Stratagene). The quantity of gene expression was generated by comparison of the fluorescence generated by each sample with standard curves of known quantities, and the calculated number of copies was divided by the number of copies of the housekeeping gene *Gapdh* (encoding glyceraldehyde phosphate dehydrogenase) or *B2m* (encoding β_2-microglobulin).

Uptake of apoptotic cells *in vitro* and *in vivo*. DCs, macrophages and neutrophils were isolated from *Scarf1*$^{+/+}$ and *Scarf1*$^{-/-}$ mice with EasySep magnetic isolation kits according to the manufacturer's instructions (STEMCELL Technologies). Those cells were incubated for 0.5, 1, or 2 h at 37 °C with CFSE- or pHrodo-labeled apoptotic cells. Cells were stained with fluorescence-labeled anti-CD11c (N418; eBioscience), anti-Ly6G (RB6-8C5; eBioscience), anti-F4/80 (BM8; eBioscience), anti-CD11b (M1/70; eBioscience) and anti-CD8α (53-6.7; eBioscience) and were analyzed by flow cytometry. For *in vivo* assays of the uptake of apoptotic cells, dye-labeled apoptotic B cells or MEFs were injected intravenously into *Scarf1*$^{+/+}$ and *Scarf1*$^{-/-}$ mice. After 1 h, spleens were collected and the CD11c$^+$ DC population was isolated by negative selection with an EasySep kit. The enriched DC population was stained with fluorescence-labeled anti-CD11c (N418; eBioscience) and anti-CD8α (53-6.7; eBioscience). Splenocytes that took up pHrodo-labeled MEFs by phagocytosis had a change in florescence from 488 nm (fluorescein isothiocyanate) to 550 nm (phycoerythrin). Samples were analyzed with FACSCalibur (Becton Dickinson) and data were collected with CellQuest Software and analyzed with FlowJo 9.5 version for Mac (TreeStar).

Autoantibody profiles. ANA and *C. luciliae* immunofluorescence assays were done according to the manufacturer's instructions (Bio-Rad) with mouse serum at a dilution of 1:160 to 1:5120 and *C. luciliae* at a dilution of 1:50 to 1:200 dilutions. Staining was scored by an observer 'blinded' to the genotypes of the mice. For ELISA of nucleosomes, smRNP or the nuclear protein La, polystyrene plates were coated with dsDNA and histones, smRNP-complex antigens or La, respectively (Immunovision). After blockade of nonspecific binding with 1% BSA in PBS, serial dilutions of serum from 1:160 to 1:5120 were added. Specific antibodies were detected with horseradish persoxidase–conjugated goat anti-mouse IgG (HAF007; R&D Systems), and absorbance at 405 nm and 630 nm was compared with that of positive control serum (Immunovision) for quantification.

TUNEL assay. Frozen sections were allowed to warm to 25 °C. A TUNEL assay (terminal deoxynucleotidyl transferase-mediated dUTP nick end-labeling) for the detection of apoptotic cells was done according to manufacturer's instructions (Invitrogen). Paraformaldehyde-fixed tissue was made permeable with 0.25% Triton X-100 in PBS and was washed twice with PBS. Slides were incubated with reaction buffer (25 mM Tris-HCl, pH 6.6, 200 mM sodium cacodylate, 0.25 mg/ml BSA and 1 mM cobalt) containing terminal deoxynucleotidyl transferase, then were washed twice and were incubated for 45 min at 25 °C in the dark (protected from light) with reaction buffer containing the fluorescent label Alexa Fluor 488. Actin filaments of the cells were stained for 10 min at 25 °C with Alexa Fluor 546–anti-phalloidin (1:500 dilution; A22283; Invitrogen) in PBS. Samples were washed twice with PBS. Finally, DNA was stained for 10 min at 25 °C with Hoechst 33342 (1:1,000 dilution; Molecular Probes, Invitrogen). Slides were mounted with Vectamount mounting medium (Vector Laboratories) and were visualized with a Nikon Eclipse ME600 fluorescent microscope equipped with a high-resolution DXM1200C Nikon digital camera. Data were analyzed with NIS-Elements software (Nikon) and Adobe Photoshop.

Immunocomplex imaging. Frozen sections were allowed to warm to 25 °C and then were fixed with 4% paraformaldehyde. Slides were washed twice with PBS at 25 °C; each wash was done for 5 min to allow tissue rehydration. After that step, nonspecific binding of slides was blocked for 45 min at 25 °C with PBS supplemented with 10% goat serum (Invitrogen). PBS washed slides were stained for 20 min at 25 °C in the dark (protected from light) with Alexa Fluor 488–conjugated goat antibody to mouse IgG (1 μl per slide; A11001; Invitrogen) After being stained, slides were washed twice, mounted with Vectashield containing DAPI (4,6-diamidino-2-phenylindole) and visualized by fluorescent microscopy.

Production of and infection with lentivirus. Plasmids encoding lentivirus expressing shRNA molecules were obtained from The RNAi Consortium shRNA Library (Broad Institute). The shRNA targeting 21-nucleotide sequences were as follows: shControl, CCTAAGGTTAAGTCGCCCTCG; shC1q 1, CGGCTTCTATTACTTCAACTT; shC1q 2, CCTGAGTTTCTCTAACACCAA; shC1q 3, CGACAGCATCTTCAGCGGATT; and shC1q 4, GCTTGGCAA CGTGGTTATCTT. Plasmids were purified with a QIAprep Miniprep kit (Qiagen) and then were used for transfection of HEK293T cells along with pCMV-dR8.2 dvpr and pCMV-VSVG for the production of lentivirus. MEFs were placed in 24-well tissue culture dishes (2×10^5 cells per well) and infected with 100 μl unconcentrated shRNA lentiviral supernatant and polybrene (7.5 μg/ml). Cells were spun for 30 min at 800*g*, then the medium replaced, followed by incubation for 2 d. Infected cells were selected in complete RPMI medium containing 10% (vol/vol) FBS and puromycin (3 μg/ml) and were tested 1 week after infection. The knockdown efficiency of shRNA was determined by quantitative PCR.

Histological assessment and clinical disease scores. Histopathologic examination of skin, spleen and kidney samples was done after routine fixation of the tissues and embedding in paraffin. Tissue sections were cut from the skin and stained with hematoxylin and eosin. All slides were coded and evaluated by researchers 'blinded' to the identity of the sample. The severity of skin inflammation was assigned a score on a scale of 0–4 as follows: 0, normal; 1, hyperplasia of the epidermis; and 2–4, increasing numbers of infiltrating inflammatory cells in the skin. Mice were also assigned scores for the extent of lesions on the face, ears, head, neck and back. Macroscopic surface area was assigned a score on a scale of 0–4 as follows: 0, normal; 1, mild lesion; and 2-4, increasing severity of lesion and loss of hair and whiskers from the affected area up to 2 cm^2. A composite score of skin disease was generated from the microscopic and macroscopic analyses. Pathological changes in the kidney were assigned 'grades' according to the presence of glomerular, interstitial or perivascular inflammation and deposition of immunocomplexes. Scores ranging from 0 (normal) to 4 (most severely inflamed) were assigned for each of the four features. A minimum of 50 glomeruli were assessed to determine the glomerular index in each mouse.

Assessment of urine. Mice in each group were placed for 24 h in sterilized Nalgene metabolic cages for the collection of urine. Chemstrip 5OB test strips (Roche) were used for urinalysis. Proteinuria was assigned 'grades' on a scale of 0–4 as follows: 0, none; 1, 30–100 mg/dl; 2, 100–300 mg/dl; 3, 300–2,000 mg/dl; and 4, >2,000 mg/dl.

Statistical analysis. Statistical calculations were done with a statistical software package (GraphPad Prism 5.0d). For comparisons of two groups, the mean ± s.e.m. was analyzed by the two-tailed unpaired Student's *t*-test with the Bonferroni correction applied for multiple comparisons. For comparisons of more than two groups, significance was determining with the one- or two-way analysis of variance with correction. The investigators were not blinded to the genotype of the mice except where indicated. Samples sizes were selected on the basis of preliminary results to ensure a power of 80% with 95% confidence between populations.

doi:10.1038/ni.2670